



HAL
open science

A new method for evaluation of antifouling activity of molecules against microalgal biofilms using confocal laser scanning microscopy-microfluidic flow-cells

Karine Rehel, Isabelle Linossier, Tiffany Le Norcy, Fabienne Fay, Claudia Zea Obando, Claire Hellio

► To cite this version:

Karine Rehel, Isabelle Linossier, Tiffany Le Norcy, Fabienne Fay, Claudia Zea Obando, et al.. A new method for evaluation of antifouling activity of molecules against microalgal biofilms using confocal laser scanning microscopy-microfluidic flow-cells. *International Biodeterioration and Biodegradation*, 2019, 139, pp.54-61. 10.1016/j.ibiod.2019.03.001 . hal-02871384

HAL Id: hal-02871384

<https://hal.science/hal-02871384v1>

Submitted on 22 Oct 2021

HAL is a multi-disciplinary open access archive for the deposit and dissemination of scientific research documents, whether they are published or not. The documents may come from teaching and research institutions in France or abroad, or from public or private research centers.

L'archive ouverte pluridisciplinaire **HAL**, est destinée au dépôt et à la diffusion de documents scientifiques de niveau recherche, publiés ou non, émanant des établissements d'enseignement et de recherche français ou étrangers, des laboratoires publics ou privés.



Distributed under a Creative Commons Attribution - NonCommercial 4.0 International License

1 **A new method for evaluation of antifouling activity of molecules against microalgal biofilms**
2 **using Confocal Laser Scanning Microscopy-Microfluidic Flow-cells.**

3
4 Tiffany Le Norcy¹, Fabienne Fay^{1*}, Claudia Zea Obando¹, Claire Hellio², Karine Réhel¹, Isabelle
5 Linossier¹

6 1. Univ. Bretagne-Sud, EA 3884, LBCM, IUEM, F-56100 Lorient, France
7 fabienne.fay@univ-ubs.fr

8 2. Biodimar, LEMAR UMR 6539, Institut Européen de la Mer, Université de Bretagne
9 Occidentale, 29200 Brest, France

10

11 **Abstract**

12 Regulatory developments regarding antifouling molecules encourage the search for non-toxic
13 substances. Evaluation tools must evolve to highlight anti-adhesion effects rather than growth
14 inhibition. The work presented here aimed at developing a method based on confocal laser scanning
15 microscopy-microfluidic flow-cells in order to characterize microalgal biofilms. The first part of
16 the work was dedicated to the setting-up of experimental parameters allowing the production of
17 microalgal biofilms. The results obtained showed that it was indeed possible to produce
18 reproducibly biofilms. The size of microalgal strains appeared to be a key-parameter in the
19 adhesion rate and cells adhesion strength. *Cylindrotheca closterium* cells adhered in lower amount
20 but formed denser biofilms than *Porphyridium purpureum*. The second part of the work focused
21 on the evaluation of a known antifouling molecule, dibromohemibastadin-1 (DBHB). A
22 comparison with the conventionally used method, multi-well plates experiments, was established.
23 The multi-well plates experiments allowed the determination of minimum inhibitory concentration
24 (MIC) for growth and adhesion inhibition (around 80 μ M). The flow-cells combined with confocal
25 laser scanning microscopy (CLSM) enabled the observation of biofilm, the determination of
26 kinetics parameters of adhesion and an estimation of the adhesion strength.

27

28 **Keywords:** Microalgae, flow-cell, adhesion, biofilm, CLSM, multi-well plate, bioassay,
29 antifouling, methodology, *Cylindrotheca closterium*, *Porphyridium purpureum*.

30

31

32 **1. Introduction**

33 Biofilms consists of agglomerates of microorganisms surrounded by a self-produced extracellular
34 matrix (ECM) composed primarily of extracellular polymeric substances (EPS). In seawater,
35 biofilms on submerged surfaces are mainly composed of bacteria and microalgae (Wahl 1989,
36 Cooksey and Wigglesworth-Cooksey1995, Dang and Lowell 2016). These complex structures
37 have been observed by sampling biofilms from various substrates collected in the marine
38 environment (Arrhenius *et al.* 2014, Maso *et al.* 2016, Faÿ *et al.* 2018, Balqadi *et al.* 2018) or by
39 using laboratory methods combining culture and imaging of biofilms (Doiron *et al.* 2012, Reddy
40 *et al.* 2017, He *et al.* 2016, Di Peppo and Congestri, 2017). Indeed, the characterization of biofilms
41 in terms of composition and structure has been made possible by the development of 3-D mapping
42 techniques associated with confocal laser scanning microscopy (CLSM). This method has been
43 extensively used in the studies of bacterial biofilm formation (Azerdo *et al.* 2017, Pamp 2009, Arai
44 *et al.* 2015, Smaldone *et al.* 2014, Haagensen *et al.* 2015), cyanobacteria (David *et al.* 2015) and
45 natural communities (Larson and Passy 2005, Proia *et al.* 2012, Mueller *et al.* 2006, Risse-Buhl *et al.*
46 *et al.* 2017). The use of microfluidics associated with CLSM is particularly interesting to study
47 microbial adhesion and detachment, biofilm integrity and structural parameters (biomass, thickness
48 and cell viability), as well as biofilm susceptibility to antibiotics (Macia and al. 2014, Pousti *et al.*
49 2019). Direct real-time non-destructive visualization of biofilms developed on substrata informs
50 on spatial relationships between organisms as well as with substrata. Nevertheless, the use of flow-
51 cell systems associated with CLSM to observe mono-species microalgal biofilms is so far poorly
52 described (Irving and Allen 2011, Ozkan 2013a). Most of the studies concerning microalgae focus
53 on the design of devices dedicated to biomass and lipid productions, and, treatment of wastewaters
54 (Berner *et al.* 2014, Katarzyna *et al.* 2015, Bruno *et al.* 2012, Boelee *et al.* 2011, Gismondi *et al.*
55 2016, Chaudhary *et al.* 2017). Hence, the first objective of this paper was to determine experimental
56 parameters suitable to obtain *in vitro* microalgal biofilms in flow cell by using a system adapted
57 from the protocol of Sternberg and co-workers (Sternberg *et al.* 2006, Tolker-Nielson and
58 Steinberg 2011, Pamp *et al.* 2009). For this, two model microalgae strains were used:
59 *Cylindrotheca closterium* (Bacillariophyceae) and *Porphyridium purpureum*
60 (Porphyridiophyceae). Both strains were chosen because they are involved in colonization of

61 marine substrates (Jellali et al. 2013) and are commonly studied in colonization assessment (Briand
62 *et al.*, 2012, Zargiel and Swain 2014). They are associated with strong adhesion on surfaces and
63 play an important role as exopolysaccharides producers within biofilms (Staats et al 1999, Zaouk
64 et al. 2018). Thus, inhibition of the adhesion of these strains is a real challenge for the maritime
65 industries, especially because they can be as well involved in biocorrosion (Landousli et al., 2011).

66 In addition, in the context of antifouling coatings and ever more pressing regulatory constraints
67 (for example, EU Biocidal Product Regulation EU 528/2012) the development of tools for
68 assessing anti-bioadhesion molecules is essential. The second part of this study consisted of using
69 the method previously developed to evaluate a known antifouling molecule dibromohemibastadin-
70 1 (DBHB) (Bayer *et al.* 2011, Niemann *et al.* 2015, Ortlepp *et al.* 2007, Le Norcy *et al.* 2017a) in
71 comparison with the reference method (multi-well plates). Generally, microplates or classical
72 microbiological techniques are used to determine minimum inhibitory concentrations (MIC) of
73 compounds against bacteria and microalgae (Plouguerne *et al.* 2010, Iyapparaj and al. 2014,
74 Prakash *et al.* 2015, Gao *et al.* 2014, Bressy et al 2014). However, with these technics, only the
75 impact of compounds on the growth or toxicity can be evaluated and only few papers have studied
76 the impact of compounds on adhesion (Jin *et al.* 2014, Xin *et al.* 2017, Abed *et al.* 2013). In this
77 paper, the impact of a reference compound on cell adhesion, adhesion strength and cell growth rate
78 on surfaces was studied *via* the CLSM-Microfluidic Flow-cells method.

79

80 **2. Materials and Methods**

81 **2.1 Strains**

82 Microalgal strains were obtained from Algotank (Biological Resource Center of the University of
83 Caen Normandie, France): *Cylindrotheca closterium* (AC-170) (Bacillariophyceae, (Ehrenberg)
84 Reimann & Lewin) and *Porphyridium purpureum* (AC-122) (Porphyridiophyceae (Bory) Drew &
85 Ross).

86 **2.2 Growth**

87 Before use, strain axenisation was realized by a treatment with a mixture of three antibiotics:
88 chloramphenicol (100 µg/mL), penicillin (1000 µg/mL) and streptomycin (500 µg/mL) during 24
89 hours (Druehl and Hsiao, 1969). Both strains were grown in sterile artificial seawater (ASW, 30

90 g/L, Sigma Aldrich) supplemented with Guillard's F/2 medium at 2% (Guillard and Ryther 1962,
91 Sigma Aldrich) at 20°C. Guillard's F/2 was added after sterilisation and culture medium was stored
92 at 4°C before use. Erlenmeyer flasks were maintained under controlled illumination of 250
93 $\mu\text{mol.photons.m}^{-2}.\text{s}^{-1}$ white fluorescent lamps (Philips Master TL5 HO 54W/840 1SL/20) at 20°C
94 with a 12h:12h light:dark cycle in a Hélios 600 phytotron (Cryotec, Saint-Gély-du-Fesc, France).
95 This procedure favored the cellular growth (Forjan et al. 2005). Cultures of *C. closterium* and *P.*
96 *purpureum* were initially started with about 10^3 cell mL^{-1} . *C. closterium* reached the exponential
97 phase after 3 days, whereas *P. purpureum* needed more time (6 days). After 15 days, both strains
98 were in stationary phase. *C. closterium* showed longitudinal shape with a length of 65 ± 10 μm ,
99 whereas *P. purpureum* showed a round shape ($5\pm 0.5\mu\text{m}$) (Figure S1).

100

101 **2.3 Culture in flow-cells**

102 Microalgae were grown under hydrodynamic conditions in flow-cells. The flow-cell system was a
103 tool originally used for the *in vitro* observation of bacterial biofilm (Tolker-Nielsen and Sternberg,
104 2011) and has been adapted for microalgal biofilm observation. Microalgal biofilm was grown in
105 a three channels flow-cell (1x4x44 mm; 1.76 mL; Biocentrum, DTU, Denmark) prepared with
106 microscope glass coverslip (24x50 mm) (Knittel Glasser, Braunschweig, Germany) (Figure 1).
107 Before the experiment began, the flow-cells were sterilized by flowing a solution of sodium
108 hypochlorite (1.5%, 150 $\mu\text{L}/\text{min}$) for 1 hour. They were then rinsed by ASW supplemented with
109 Guillard's F/2 medium at 2% for 2 hours. All experiments were performed in a thermostatic stove
110 at 20°C under 12:12 h light-dark cycle at $250 \mu\text{mol.m}^{-2}.\text{s}^{-1}$. Distance between the flow cell and light
111 source (2 fluorescent tubex, T4 TL2004A, 12W, Intertek, France) was 13.5 cm.

112 *2.3.1 Adhesion of planktonic cells*

113 250 μL of microalgal culture (10^5 cells/mL) diluted in ASW supplemented with Guillard's F/2
114 medium (2%) were inoculated in each channel by using a sterile 1mL syringe. The medium flow
115 was not activated, thus allowing attachment of cells to the glass surface. Hence, the adhesion step
116 was realized in static condition. Four incubation times were studied: 8, 24, 48 and 72 hours. The
117 number of adhered cells per cm^2 after the incubation time was evaluated by CLSM observation
118 (Zeiss, LSM710) equipped with helium-neon laser source and X20 air objective. The acquisition

119 software was Zen Software (Zeiss). Cells were observed by the natural auto-fluorescence of
120 chlorophyll ($\lambda_{\text{excitation}} = 633 \text{ nm}$, $\lambda_{\text{emission}} = 638\text{--}720 \text{ nm}$). Experiments were realized with three
121 independent cultures. The three channels of each flow cell were inoculated and three randomly
122 observations were realized by channel. Hence, 27 randomly fields were considered during
123 quantification.

124 2.3.2 Growth of adhered cells

125 Biofilm maturation was evaluated after the adhesion step (24 hours without any flow of medium
126 to allow the microalgae adhesion). For this purpose, a flow (90 or 15 $\mu\text{L}/\text{min}$) was activated with
127 ASW supplemented with Guillard's F/2 medium (2%) using a Watson Marlow 205U peristaltic
128 pump (Watson Marlow, Falmouth, UK). Biofilm was observed after 24, 48, 72, 96 and 120 hours.
129 Images were taken every micrometer throughout the whole biofilm thickness. The Zen software
130 (Zeiss) was used to process data of 3D image with maximal intensity projection. The average
131 thickness of the biofilm (μm) and the biovolume ($\mu\text{m}^3/\mu\text{m}^2$) were measured using COMSTAT
132 software (Heydorn *et al* 2000). Results were representative of 27 randomly fields.

133 2.4 Evaluation of reference compound by multi-well plate assay

134 Reference compound was dibromohemibastadin-1 (DBHB). It was furnished by Prof. Proksch
135 (Institute of Pharmaceutical Biology and Biotechnology, University of Düsseldorf, Germany). It
136 was evaluated at 0.016, 1.6, 8, 16, 32 and 80 μM in 12 replicates in 96-wells microplate (black
137 with transparent base, Fisher-Scientific, Waltham, MA, USA). Methanol was used as a carrier
138 solvent to add DBHB in the microplate, and was evaporated prior to the bioassay. A well without
139 DBHB was used as control. Then, one hundred microliters microalgal cultures of 2 weeks at 10^3
140 cells/mL were added in each well and microplates were incubated at 20°C during 5 days under
141 controlled illumination ($250 \cdot \mu\text{mol} \cdot \text{photon} \cdot \text{m}^{-2} \cdot \text{s}^{-1}$) with a 12:12 light-dark cycle. The fluorescence
142 was measured ($\lambda_{\text{excitation}} = 633 \text{ nm}$, $\lambda_{\text{emission}} = 638\text{--}720 \text{ nm}$) by using a TECAN microplate
143 reader (Magellan, France) in order to quantify the total cells density in each well. Then, the
144 microplate was emptied by flipping and washed twice with ASW. The fluorescence was again
145 measured in order to quantify adhered microalgae. The difference between the total cells number
146 and the adhered cells number was calculated to obtain the number of planktonic cells. MIC was
147 defined as the lowest concentration that produced a significant reduction in growth or adhesion.
148 Experiments were repeated three times.

149

150 **2.5 Evaluation of reference compound by flow-cell assay**

151 *2.5.1 Impact on adhesion from planktonic cells*

152 The experimental procedure was the same that described above (2.3.1). The impact of compound
153 was evaluated by adding DBHB in the flow-cell at 16 or 80 μM in the microalgae inoculum
154 immediately prior to the inoculation in flow cell channels. After 24h of adhesion, the flow (120
155 $\mu\text{L}/\text{min}$) was activated during 30 minutes to remove free diatoms. The number of adhered cells was
156 compared to the control without DBHB.

157 *2.5.2 Impact on adhesion strengths*

158 The impact of DBHB on adhesion strength of microalgae was determined after the adhesion stage.
159 Experiment was realized in the presence of DBHB (16 μM) during adhesion step (72h) as described
160 above (2.5.1), then the application of a high shear stress was realized to quantify the removal
161 percentage. The flow was activated at 330 $\mu\text{L}/\text{min}$ (8.10^{-3} Pa) during 30 minutes. The cells number
162 adhered on the surface were counted again and the removal percent was determined as following:

163
$$\frac{\text{cells.cm}^{-2}_{\text{before flow}} - \text{cells.cm}^{-2}_{\text{after flow}}}{\text{cells.cm}^{-2}_{\text{before flow}}} \times 100.$$

164 The removal percentage determined for the experiment in the presence of DBHB was compared to
165 the control without DBHB.

166 *2.5.3 Impact on growth of adhered cells*

167 The impact of DBHB on biofilm maturation was evaluated by adding DBHB (16 μM) in the growth
168 medium flow. After 72 hours of adhesion without DBHB, the growth medium containing DBHB
169 was “activated” as described above (2.3.2) at 150 $\mu\text{L}/\text{min}$ during 24, 48, 72, 96 or 120 hours. The
170 biovolume and the average thickness were determined with the COMSTAT program. Experiments
171 without DBHB in the growth medium were used as control. All experiments were realized three
172 times.

173 **2.6 Statistical analysis**

174 The one-factor analysis variance (ANOVA) was used to determine the effect of studied conditions.

175 The level of significance was set to $p < 0.01$. Values were means \pm standard deviation (sd).

176

177 **3 Results and discussion**

178 **3.1 Culture of microalgal biofilm in flow-cell system.**

179 *3.1.1 Adhesion from planktonic cells*

180 Figures 2 and S2 show the adhesion kinetics of *C. closterium* and *P. purpureum* in flow-cells over
181 72 hours. The count represents the number of cells irreversibly adhered. Single cells were observed
182 on the totality of the cover glass, which indicated that initial attachment of cells was homogeneous.
183 However, the adhered cells number for both strains was significantly different. The number of
184 adhered cells increased with the time: a significant ($p < 0.01$) difference was observed between each
185 observation. For *C. closterium*, the results indicated that the rate of adhesion to glass can be divided
186 in 3 parts: 1) during the first 8 hours, the density increased with a rate of 1280 cells/cm²/h, 2) the
187 rate decreased to 330 cells/cm²/h during the subsequent 48 hours ($r^2 = 0.9998$), and 3) finally in the
188 last 24 hours the rate decreased further to 65 cells/cm²/h. This profile of cells multiplication on
189 glass slide has been already shown for *Chlorella vulgaris* (Ozkan *et al.* 2013a). For *P. purpureum*,
190 the rate adhesion rate showed only 2 parts: after a high adhesion rate during the first 8 hours (2145
191 cells/cm²/h), a linear rate ($r^2 = 0.9989$) of 555 cells/cm²/h was observed to the end of the
192 experiment.

193 Cells densities ($2.5 \cdot 10^4$ and $5.1 \cdot 10^4$ cells/cm² respectively at 72h) were significantly different (p
194 < 0.01) for *C. closterium* and *P. purpureum*. This observation could be explained by the
195 morphology of microalgae. *C. closterium* is elongated (65 μm) whereas *P. purpureum* is spherical
196 and smaller (5 μm diameter). For an equal space and for reasons of steric constraints, more *P.*
197 *purpureum* cells are likely to adhere than *C. closterium* cells. These results were consistent with
198 the observation of Sekar *et al.* (2004), who indicated variability in the microalgal adhesion levels
199 and an increase of adhesion with exposure time.

200

201

202 *3.1.2 Growth of adhered cells*

203 Biofilm formation of *C. closterium* and *P. purpureum* was evaluated under constant flow
204 conditions, after the step of adhesion (24h). In the case of bacteria, it has been established that two
205 factors influenced the structure of biofilms and needed to be controlled: the flow velocity and the
206 nutrient status. Indeed, the flow velocity determined the hydrodynamic shear and the mass transfer
207 characteristics of a system (Stoodley *et al.* 1999). Hence, microalgal biofilms were grown during
208 application of a continuous flow (90 or 150 $\mu\text{L}/\text{min}$) in the presence of medium culture (ASW
209 supplemented with Guillard's F/2). Microalgal biovolume was quantified during 120 hours and the
210 growth kinetics was determined (Figure 3). The cellular density increased with time and the
211 medium flow velocity. As for bacteria, an increase of fluid flow velocity in the flow-cells resulted
212 in faster development of microorganisms due to higher nutrients transport (Bussher and van der
213 Mei 2006). For both strains, the biovolume increased linearly with time after 48 hours of medium
214 flow which indicated a cellular multiplication at a constant rate during the time of experiment. In
215 the case of *C. closterium* a time lag was observed. Then, a growth rate could be determined. Results
216 showed a significant higher ($p < 0.01$) growth rate at a flow velocity of 150 $\mu\text{L}/\text{min}$ (0.1102
217 $\mu\text{m}^3/\mu\text{m}^2/\text{h}$) compared to the flow velocity at 90 $\mu\text{L}/\mu\text{min}$ ($0.0612 \mu\text{m}^3/\mu\text{m}^2/\text{h}$). The biomass
218 reached after 120 hours a value significantly higher ($9.1 \mu\text{m}^3/\mu\text{m}^2$ versus $5.5 \mu\text{m}^3/\mu\text{m}^2$
219 respectively). For *P. purpureum*, no time lag was observed. The cellular multiplication took place
220 mainly in the first 48 hours, then a decrease of cellular multiplication was observed indicating the
221 end of the maturation process: the increase in the cells number between two times was not
222 significant ($p > 0.05$). Moreover, the impact of flow velocity was not significant ($p > 0.05$): similar
223 growth rates ($0.0083 \mu\text{m}^3/\mu\text{m}^2/\text{h}$) were determined. On the other hand, the biovolume was
224 significantly ($p < 0.01$) higher for *C. closterium*: the denser biofilm was obtained for a flow velocity
225 of 150 $\mu\text{L}/\text{min}$. This result could be explained by the size of cells and their respective growth rates
226 (10 times greater on average for *C. closterium*).

227 The microscopic observations of biofilms developed during 48, 72, 96 and 120 hours at a flow
228 velocity of 150 $\mu\text{L}/\text{min}$ are shown in Figure 4A. The qualitative results described the spatial
229 organization of microalgae in biofilm: cells agglomerated to each other and at the glass surface.
230 Results showed the capability of *C. closterium* and *P. purpureum* to form a biofilm in flow-cell
231 experiment after 120 hours. Nevertheless, the structure of biofilm was dependent on the strain
232 studied. In the case of *C. closterium* biofilms, cells formed dense aggregates, whereas in *P.*
233 *purpureum* biofilms cells were more scattered. Based on the biofilm image analysis, biovolumes

234 were quantified for each strain and results are shown Figure 4B. Biofilm formation was highly
235 repeatable between independent experiments (standard deviation lower than $1 \mu\text{m}^3/\mu\text{m}^2$ and 0.2
236 $\mu\text{m}^3/\mu\text{m}^2$ for *C. closterium* and *P. purpureum* biovolume respectively). However, the observed
237 biofilms indicated average thicknesses relatively low ($< 40 \mu\text{m}$) (Figure 4C) compared to those of
238 millimeters or more observed in natural environment (Irvin *et al.* 2011). The biofilm observed for
239 *C. closterium* was denser ($9.1 \mu\text{m}^3/\mu\text{m}^2$) and thicker ($38 \mu\text{m}$) than for *P. purpureum* which
240 indicated only $1.5 \mu\text{m}^3/\mu\text{m}^2$ and $10.2 \mu\text{m}$ for biovolume and average thickness respectively. *C.*
241 *closterium* covered more quickly the surface, then cells adhered to each other to form a 3D structure
242 (from 72 h). Another species of the genus *Cylindrotheca* (*C. fusiformis*) was identified as excellent
243 candidates to form biofilms due to their strong attractiveness to glass but also cell to cell
244 interactions (Ozkan *et al.* 2013b). On the contrary, *P. purpureum* developed longitudinally on the
245 surface. A relatively homogeneous surface pattern interspersed with a few macro-colonies was
246 observed after 120 hours. These differences could be explained in particular by the size of cells.

247

248 **3.2 Use of culture in flow-cells to evaluate antibiofilm/ anti-bioadhesion compounds**

249 The use of bioassays to evaluate anti-biofilms compounds is essential to screen potential substances
250 and understanding their mode of action. Among bioassays developed, the use of multiwell plates
251 is particularly common (Trepas *et al.* 2014, Hellio *et al.* 2015). However, biofilms developed in
252 flow-cells could also be useful to evaluate the anti-microbial biofilm activity of compounds (Table
253 1). Data obtained with both bioassays are listed in Table 2 and it appeared clearly that study in flow
254 cells led deeper analysis.

255 In this context, a reference compound has been tested using both bioassays: multi-well plates and
256 flow-cell system. A hemibastadin analog named dibromohemibastadin-1 was selected. It has been
257 shown an anti-bacterial biofilm and anti-quorum sensing activities without toxic activity (Le Norcy
258 *et al.* 2017a). DBHB can inhibit the settlement of cyprid larvae of *Balanus improvisus* and byssus
259 formation of *Mytilus edulis* without toxicity on nauplii of *Artemia salina* (Bayer *et al.* 2011,
260 Niemann *et al.* 2015, Ortlepp *et al.* 2007). Moreover, on four species tested, DBHB affected the
261 growth of two microalgae (*C. closterium* and *Exanthemachrysis gayraliae*) with a MIC of $80 \mu\text{M}$
262 after 5 days (Le Norcy 2017b).

263

264 3.2.1 Study of DBHB by multi-well plates

265 DBHB activity (at concentration from 0.016 to 80 μM) was evaluated towards microalgal adhesion
266 and growth and MIC values were determined. MIC is defined as the lowest concentration that
267 produces a significant reduction in growth or adhesion (Hellio *et al.* 2015). Strains showed different
268 sensitivity to DBHB. DBHB exhibited an inhibitory activity against *C. closterium* (80 μM) in terms
269 of both growth and adhesion whereas *P. purpureum* displayed a lower sensitivity towards DBHB
270 (no inhibition up to 80 μM). This result correlated well with previous studies using the same
271 bioassay for the screening of natural antifoulants: *P. purpureum* was described as a resisting strain
272 (Moodie *et al.* 2018).

273

274 3.2.2 Impact of DBHB on adhesion of planktonic cells by flow-cells

275 From results obtained using multi-well plates, the evaluation of DBHB activity against microalgal
276 adhesion was realized by using flow-cell system. It was operated at two concentrations: 16 and 80
277 μM . At 16 μM , no impact on the microalgal growth was observed in multi-well plates whereas 80
278 μM corresponding to the MIC.

279 The impact of DBHB on *C. closterium* and *P. purpureum* is evaluated (Figure S3). For this purpose,
280 DBHB (16 or 80 μM) was injected in the flow cell at the same time as microalgal cells. After 24
281 hours of static adhesion, a difference of adhesion was observed between both strains. DBHB did
282 not affect the *P. purpureum* adhesion at the tested concentrations. Concerning, *C. closterium* a
283 significant ($p < 0.01$) decrease of adhesion was observed for a concentration of 80 μM whereas for
284 16 μM , no significant effect ($p > 0.05$) was observed on the number of adhered cells. All results
285 corroborated with those mentioned above. However, it could be pointed out that for *C. closterium*,
286 in the presence of 80 μM , the inhibition rates diverged: inhibition percentages of 100% and 40%
287 (comparatively to control) were quantified for multi-well plates and flow-cell bioassay,
288 respectively. The adhesion of cells was influenced by several parameters. For example, the
289 adhesion surface (polystyrene versus glass), the physiological state of cells during experiment (5
290 days versus 24 hours), the inoculation cellular concentration (10^3 vs 10^5 cells/mL), the washing

291 method (pipette versus peristaltic pump) were parameters that could impact microalgal adhesion
292 evaluation.

293

294 3.2.3 Impact of DBHB on adhesion strengths in flow-cells

295 The use of flow-cells allowed the determination of the impact of DBHB on the adhesion strengths
296 of microalgae. For that, after 72 hours of adhesion in flow cells with DBHB, a continuous flow
297 (330 $\mu\text{L}/\text{min}$, 8.10^{-3} Pa) was applied during 30 minutes. The concentration of 16 μM was applied
298 to be lower than the MIC (80 μM). The number of adhered cells on glass slide was quantified before
299 and after activation of flow and the removal percentage was determined. These data provided key
300 information about adhesion strengths of cells on the glass surface which increased with time as
301 observed in previous studies (Schultz et al. 2000, Holland *et al.* 2004, Finlay *et al.* 2013, Alles and
302 Rosenhahn 2015, Nolte et al 2017). Concerning *C. closterium*, a significant ($p < 0.01$) increase of
303 removal percent was observed after 72 hours in the presence of DBHB (from $24 \pm 4\%$ to $41 \pm 2\%$):
304 the adhesion strengths were lesser. This result was particularly interesting because *C. closterium* is
305 a large diatom. It has been shown that the magnitude of interactions (as electrostatic, van de Waals
306 and acid base) increased with increasing cell size. Moreover, the drag forces acting on cells
307 augmented with increasing cell size in systems involving medium flow (Ozkan *et al.* 2013b). For
308 *P. purpureum*, no significant difference was observed between the standard and the experiment
309 containing DBHB. DBHB did not act in the same way against *C. closterium* than *P. purpureum*.
310 The adhesion of microalgae was strongly linked to the physico-chemical attraction between
311 microalgal cells containing bound extracellular polymeric substances and the substratum (Klein *et*
312 *al.* 2014, Ozkan *et al.* 2013a). Hypothetically, DBHB could affect these parameters disturbing not
313 only the number of adhered cells but also their adhesion strengths. Hence, flow cell bioassay could
314 inform not only on the ability of bioactive compounds to inhibit the adhesion but also on
315 mechanisms of action of bioactive compounds.

316

317 3.2.4 Impact of DBHB on growth of adhered cells in flow cell

318 To evaluate the impact of DBHB on the growth of adhered cells, the compound in solution (at 16
319 μM) was added in the growth medium. After application of a continuous flow, the biovolume

320 developed on glass slide was quantified. Two different behaviors were observed depending on the
321 strains.

322 For *C. closterium*, no cell was observed after 24 hours. Cells previously adhered in flow cell system
323 were probably detached from glass surface in the presence of DBHB and the application of flow.
324 Results confirmed those mentioned above: DBHB decreased *C. closterium* adhesion strengths.

325 For *P. purpureum* no effect of DBHB was observed. Whatever the incubation time tested, the
326 biovolume developed in the presence of 16 μ M DBHB was not significantly different ($p>0.05$)
327 from control (Figure S4). This result was in accordance with results obtained in multi-well plates:
328 DBHB did not affect *P. purpureum* growth.

329

330 **4. Conclusion**

331 The results of our experiments have shown the ability of microalgae to form biofilms in flow-cells.
332 *P. purpureum* cells adhered in higher number on glass surfaces than *C. closterium* cells.
333 Nevertheless, *C. closterium* formed thicker biofilms. The results corroborated those obtained with
334 the reference method (multiwell plate). However, flow-cell system was able to discriminate the
335 adhesion of planktonic cells and the growth of adhered cells contrary to multi-well plate assay.
336 Additional data could also be obtained as the impact of compounds on adhesion strengths and the
337 morphology of biofilms. The flow-cell system appeared to be a complementary method to multi-
338 well plate assay, which remains a first essential step for the screening of potential antibiofilm
339 compounds. This method is more informative but it is nonetheless more difficult to implement,
340 requires more compound and especially requires a confocal laser scanning microscope to provide
341 biofilms structural observations and digital data as biovolume. The method can be applied in the
342 research of antibiofilm/antifouling compounds (natural substances, commercial organic biocides)
343 used in antifouling paint as well as in other domains impacted by biofilms development (water
344 treatment, fish farming, industrial processes...). Biochemical process and mechanisms could be
345 evaluated in further works to improve the current knowledge.

346

347

348 **Acknowledgements:** The authors acknowledge the financial support for the PhD of T. Le Norcy:
349 Région Bretagne (ARED LACTOPAI) and the Université de Bretagne occidentale. Authors are
350 gratefully acknowledged to Prof Peter Proksch (Institute of Pharmaceutical Biology and
351 Biotechnology, University of Düsseldorf, Germany) for allowing the study on DBHB by the
352 synthesis of the molecule.

353

354 **Declaration of interest:** none

355

356 **References**

- 357 Abed, R.M.M., Dobretsov, S., Al-Fori, M., Gunasekera, S.P., Sudesh, K., Paul, V.J., 2013,
358 Quorum-sensing inhibitory compounds from extremophilic microorganisms isolated from
359 a hypersaline cyanobacterial mat. *J Industrial Microbiology & Biotechnology* 40, 759-772.
- 360 Alles, M., Rosenhahn, A., 2015. Microfluidic detachment assay to probe the adhesion of diatoms.
361 *Biofouling* 31, 469-480.
- 362 Arai, T., Ochiai, K., Senpuku, H., 2015. *Actinomyces naeslundii* GroEL-dependent initial
363 attachment and biofilm formation in a flow cell system. *Journal of Microbiological*
364 *Methods* 109, 160-166.
- 365 Arrhenius, A., Backhaus, T., Hilvarsson, A., Wendt, I., Zgrundo, A., Blanck, H., 2014, A novel
366 bioassay for evaluating the efficacy of biocides to inhibit settling and early establishment
367 of marine biofilms, *Mar. Pollut. Bull.* 87, 292–299.
- 368 Azerdo, J., Azevedo, N.F., Briandet, R., Cerca, N., Coenye, T., Costa, A.R., Desvaux, M., Di
369 Bonaventura, G., Hébraud, M., Jaglic, Z., Kacaniova, M., Knochel, S., Lourenço, A.,
370 Mergulhao, F., Meyer, R.L., Nychas, G., Simoes, M., Tress, O., Sternberg, C., 2017.
371 Critical review on biofilm methods 43, 313-351.
- 372 Balqadi, A.A., Salama, A.J., Satheesh, S., 2018. Microfouling development on artificial
373 substrates deployed in the central Red Sea. *Oceanologia*, 60, 219-231.
- 374 Bayer, M.; Hellio, C.; Maréchal, J.P.; Walter, F.; Lin, W.; Weber, H.; Proksch, P., 2011.
375 Antifouling Bastadin Congeners Target Mussel Phenoloxidase and Complex Copper(II) ions.
376 *Marine Biotechnology*, 13, 1148-1158.
- 377 Berner, F. ? Heimann, K ., Sheehan, M. 2014. Microalgal biofilms for biomass production. *J appl*
378 *Phycol* 27, 1793-1804.
- 379 Boelee, N.C., Temmink, H., Janssen, M., Buisman, C.J.N., Wijffels, R.H., 2011, Nitrogen and
380 phosphorous removal from municipal wastewater effluent using microalgal biofilms. *Water*
381 *research*, 45, 5925-5933.
- 382 Bressy, C., Briand, J.F., Compère, C., Réhel, K. 2014. Efficacy testing of biocides and biocidal
383 coatings. In *Biofouling Methods*, Dobretsov, S., Thomason, J.C., Williams, D. Eds. pp.
384 332-346. 978-0-470-65985-4
- 385 Briand, J.-F., Djeridi, I., Jamet, D., Coupé, S., Bressy, C., Molmeret, M., Le Berre, B., Rimet, F.,
386 Bouchez, A., Blache, Y., 2012. Pioneer marine biofilms on artificial surfaces including
387 antifouling coatings immersed in two contrasting French Mediterranean coast sites.
388 *Biofouling* 28, 453-463.

389 Bruno, L., Di Pippo, F., Antonaroli, S., Gismondi, A., Valentini, C., Albertano, P. 2012,
390 Characterization of biofilm-forming cyanobacteria for biomass and lipid production. *J App*
391 *Microbiology*, 113, 1052-1064.

392 Busscher, H.J., van der Mei, H.C., 2006. Microbial adhesion in flow displacement systems. *Clinical*
393 *microbiology reviews*, 19, 127-141.

394 Choudhary, P., Prajapati, S.K., Kumar, P., Malik, A., Pant, K.K. 2017, Development and
395 performance evaluation of an algal biofilm reactor for treatment of multiple wastewaters
396 and characterization of biomass for diverse applications. *Bioresource Technology*, 224,
397 276-284.

398 Cooksey, K.E., Wigglesworth-Cooksey, B., 1995. Adhesion of bacteria and diatoms to surfaces in
399 the sea: a review. *Aquatic microbial ecology*, 9, 87-96.

400 Dang, H., Lowell, C.R., 2016. Microbial surface colonization and biofilm development in marine
401 environments. *Microbiol Mol Biol Rev*, 80, 91-138.

402 David, C., Bühler, K., Schmid, A., 2015. Starilization of single species *Synechocystis* biofilms by
403 cultivation under segmented flow. *J Ind Microbiol Biotechnol*, 42, 1083-1089.

404 Di Pippo F., Congestri, R., 2017. Culturing toxic benthic blooms: the fate of natural biofilms in a
405 microcosm system. *Microorganisms*, 5, 46. doi:10.3390/microorganisms5030046

406 Doiron, K., Linossier, I., Faÿ, F., Yong, J., Wahid, E.A., Hadjiev, D., Bourgougnon, N., 2012,
407 Dynamic approaches of mixed species biofilm formation using modern technologies.
408 *Marine Environmental research*, 78, 40-47.

409 Druehl, L.D., Hsiao, S.I.C., 1969, Axenic culture of Laminariales in defined media. *Phycologia*, 8,
410 47-49.

411 Faÿ, F., Horel, G., Linossier, I., Vallée-Rehel, K. 2018, Effect of biocidal coatings on microfouling:
412 in vitro and in situ results. *Progress Organic Coatings*, 114, 162-172

413 Finlay, J.A., Schultz, M.P., Cone, G., Callow, M.E., Callow, J.A., 2013. A novel biofilm channel
414 for evaluating the adhesion of diatoms to non-biocidal coatings. *Biofouling*, 29, 401-411.

415 Forjan, E., Navarro, F., Cuaresma, M., Vaquero, I., Ruiz-Dominguez, M.C., Gojkovic, Z., Vasquez,
416 M., Marquez, M., Mogedas, B., Bermejo, E., Girlich, S., Dominguez, M.J., Vilchez, C.,
417 Vega, J.M., Garbayo, I., 2005, Microalgae: Fast-Growth sustainable Green Factories.
418 *Critical Reviews in Environmental Science and Technology*, 45, 1705-1755.

419 Gao, M., Li, F., Su, R., Wang, K., Li, X., Lu, W. 2014, Antifouling potential of the marine
420 microalga *Dunaliella salina*, *World journal of microbiology and biotechnology*, 30, 2899-
421 2905.

422 Gismondi, A., Di Pippo, F., Bruno, L., Antonaroli, S., Congestri, R. 2016, Phosphorus removal
423 coupled to bioenergy production by three cyanobacterial isolates in a biofilm dynamic
424 growth system. *Journal of Phytoremediation*, 18, 869-876.

425 Guillard, R., Ryther, J., 1962, Studies of marine planktonic diatoms, I: *Cyclotella nana* (Hustedt)
426 and *Detonula confervacea* (Cleve). *Canadian Journal of Microbiology*, 8, 229-239.

427 Haagensen, J.A.J., Hansen, S.K., Christensen, B.B., Pamp, S.J., Molin, S., 2015. Development of
428 Spatial Distribution Patterns by Biofilms Cells, *Appl Environ Microbiol*, 81, 6120-6128.

429 He, X., Wang, J., Abdoli, L., Li, H., 2016, Mg²⁺/Ca²⁺ promotes the adhesion of marine bacteria
430 and algae and enhances following biofilm formation in artificial seawater, *Colloids and*
431 *Surfaces B : Biointerfaces*, 146, 289-295.

432 Hellio, C., Trepos, R., Aguila-Ramirez, R.N., Hernandez-Guerrero, C.J. 2015, *Methods Mol Biol*,
433 1308, 421-435.

434 Heydorn, A., Nielsen, A.T., Hentzer, M., Sternberg, C., Givskov, M., Ersbøll, B.K., Molin, S.,
435 2000. Quantification of biofilm structures by the novel computer program COMSTAT.
436 *Microbiol. Read. Engl.*, 146, 2395–2407.

437 Holland, R., Dugdale, T.M., Wetherbee, R., Brennan, A.B., Finlay, J.A., Callow, J.A., Callow,
438 M.E., 2004, Adhesion and motility of fouling diatoms on a silicone elastomer, *Biofouling*,
439 20, 323-329.

440 Iyapparaj, P., Revathi, P., Ramasubburayan, R., Prakash, S., Palavesam, A., Immanuel, G.,
441 Anantharaman, P., Sautreau, A., Hellio, C., 2014, Antifouling and toxic properties of the
442 bioactive metabolites from the seagrasses *Syringodium isoetifolium* and *Cymodocea*
443 *serrulata* *Ecotoxicological and Environmental Safety*, 103, 54-60.

444 Irving, E., Allen, D.G., 2011. Species and materials considerations in the formation and
445 development of microalgal biofilms, *Appl Microbiol Biotechnol*, 92, 283-294.

446 Jellali, R., Campistron, I., Pasetto, P., Laguerre, A., Gohier, F., Hellio, C., Pilard, J.F., Mouget,
447 J.L., 2013. Antifouling activity of novel polyisoprene-based coatings made from
448 photocurable natural rubber derived oligomers. *Progress in Organic Coatings*, 76, 1203-
449 1214.

450 Jin, C., Xin, X., Yu, S., Qiu, J., Miao, L., Feng, K., Zhou, X., 2014, Antidiatom activity of marine
451 bacteria associated with sponges from San Juan Island, Washington. *World Journal of*
452 *Microbiology and Biotechnology*, 30, 1325-2334.

453 Katarzyna, L., Sai, G., Singh O. A., 2015, Non-enclosure methods for non-suspended microalgal
454 cultivation: literature review and research needs. *Renewable and sustainable energy*
455 *reviews*, 42, 1418-1427.

456 Klein, G.L., Pierre, G., Bellon-Fontaine, M.N., Zhao, M., Breret, M., Maugard, T., Graber, M.,
457 2014, Marine diatom *Navicula jeffreyi* from biochemical composition and physico-
458 chemical surface properties to understanding the first step of benthic biofilm formation.
459 *Journal Adhesion Science and Technology*, 28, 1739-1753.

460 Landoulsi, J., Cooksey, K.E., Dupres, V., 2011, Review – Interactions between diatoms and
461 stainless steel: focus on biofouling and biocorrosion. *Biofouling*, 27, 1105-1124.

462 Larson, C., Passy, S.I., 2005. Spectral fingerprinting of algal communities: a novel approach to
463 biofilm analysis and biomonitoring, *J Phycol*, 41, 439-446.

464 Le Norcy, T., Nieman, H., Proksch, P., Tait, K., Linossier, I., Réhel, K., Hellio, C., Fayé, F., 2017a,
465 Sponges-Inspired Dibromohemibastadin Prevents and Disrupts bacterial biofilms without
466 toxicity, *Marine Drugs*, 15, 222.

467 Le Norcy, T., Nieman, H., Proksch, P., Linossier, I., Vallée-Réhel, K., Hellio, C., Fayé, F., 2017b,
468 Anti-biofilm effect of biodegradable coatings based on hemibastadin derivative in marine
469 environment, *International Journal Molecular Sciences*, 18, 1520.

470 Macia, M.D., Rojo-Molinero, E., Oliver, A. 2014. Antimicrobial susceptibility testing in biofilm-
471 growing bacteria. *Clinical Microbiology and Infection*, 20, 981-990.

472 Maso, M., Fortunato, J.M., de Juan, S., Demestre, M. 2016. Microfouling communities from pelagic
473 and benthic marine plastic debris sampled across Mediterranean coastal waters. *Scientia*
474 *Marina* 80S1, 117-127.

475 Moodie, L.W.K., Cervin, G., Trepos, R., Labriere, C., Hellio, C., Pavia, H., Svenson, 2018, J.
476 Design and biological evaluation of antifouling dihydrostilbene oxime hybrids, *Marine*
477 *Biotechnology*, 20, 257-267.

478 Mueller, L.N., de Brouwer, J.F.C., Almeida, J.S., Stal, L.J., Xavier, J.B., 2006, *BMC Ecology* 6,
479 1-15.

480 Niemann, H.; Hagenow, J.; Chung, M.Y.; Hellio, C.; Weber, H.; Proksch, P., 2015. SAR of
481 Sponge-Inspired Hemibastadin Congeners Inhibiting Blue Mussel PhenolOxidase, *Marine*
482 *Drugs*, 13, 3061-3071.

483 Nolte, K.A., Schwarze, J., Rosenhahn, A., 2017. Microfluidic accumulation assay probes
484 attachment of biofilm forming diatom cells. *Biofouling*, 33, 531-543.

485 Ortlepp, S.; Sjögren, M.; Dahlström, M.; Weber, H.; Ebel, R.; Edrada, R.; Thoms, C.; Schupp, P.;
486 Bohlin, L.; Proksch, P., 2007. Antifouling Activity of Bromotyrosine-derived Sponge
487 Metabolites and Synthetic Analogues, *Marine Biotechnology*, 9, 776-785.

488 Ozkan, A., Berberoglu, H., 2013a. Adhesion of algal cells to surfaces. *Biofouling* 29, 469-482.

489 Ozjkan, A.; Berberoglu, H., 2013b. Cell to substratum and cell to cell interactions of microalgae.
490 *Colloids and surfaces B: Biointerfaces*, 2013, 302-309.

491 Pamp, S.J., Sternberg, C., Tolker-Nielson, T., 2009. Insight into the microbial Multicellular
492 Lifestyle *via* Flow-Cell Technology and Confocal Microscopy. *Cytometry*, 75A, 90-103.

493 Plouguerne, E., Ioannou, E., Georgantea, P., Vagias, C., Roussis, V., Hellio, C., Kraffe, E., Stiger-
494 Pouvreau, V., 2010. Anti-microfouling activity of lipidic metabolites from the invasive
495 brown alga *sargassum muticum* (yendo) fensholt. *Marine biotechnology*, 12, 52-61.

496 Pousti, M., Zarabadi, M.P., Amirdehi, M.A., Paquet-Mercier, F., Greener, J., 2019. Microfluidic
497 bioanalytic flow cells for biofilm studies: a review. *Analyst*, 144, 68-86.

498 Prakash, S., Ramasubburayan, R., Iyapparaj, P., Arthi, A.P.R., Ahila, N.K., Ramkumar, V.S.,
499 Immanuel, G., Palavesam, A., 2015. Environmentally benign antifouling potentials of
500 triterpene-glycosides from *Streptomyces fradiae*: a mangrove isolate. *RSC Adv.*, 5, 29524-
501 29534.

502 Proia, L., Romani, A.M., Sabater, S., 2012. Nutrients and light effects on stream biofilms: a
503 combined assessment with CLSM, structural and functional parameters. *Hydrobiologia*,
504 695, 281-291.

505 Reddy, G.K.K, Nancharaiah, Y.V., Venugopalan, V.P., 2017, Long alkyl-chain imidaolium ionic
506 liquids: antibiofilm activity against phototrophic biofilms. *Colloids and Surfaces B:*
507 *Biointerfaces*, 155, 487-496.

508 Risse-Buhl, U., Anlanger, C., Kalla, K., Neu, T.R., Noss, C., Lorke, A., Weitere, M., 2017, The
509 role of hydrodynamics in shaping the composition and architecture of epilithic biofilms in
510 fluvial ecosystems. *Water Research*, 127, 211-222.

511 Schultz, M.P., Finlay, J.A., Callow, M.E., Callow, J.A., 2000, A turbulent channel flow apparatus
512 for the determination of the adhesion strength of microfouling organisms. *Biofouling*, 15,
513 243-251.

514 Sekar, R., Venugopalan, V.P., Satpathy, K.K., Nair, K.V.K., Rao, V.N.R., 2004. Laboratory
515 studies on adhesion of microalgae to hard substrates. *Hydrobiologia*, 512, 109–116.

516 Smaldone, G.T., Jin, Y., Whitfield, D.L., Mu, A.Y., Wong, E.C., Wuertz, S., Singer, M., 2014.
517 Growth of *Myxococcus xanthus* in Continous-Flow-Cell Bioreactors as a Method for
518 studying Development. *Appl Envir Microbiology*, 80, 2461-2467.

519 Staats, N., De Winder, B., Stal, L.J., Mur, L.R., 1999, Isolation and characterization of extracellular
520 polysaccharides from the epipellic diatoms *Cylindrotheca closterium* and *Navicula*
521 *salinarum*. *Eur J Phycology*, 34, 161-169.

522 Sternberg, C., Tolker-Nielson, T., 2006, Growing and analyzing biofilms in flow cells. *Current*
523 *Protocols in Microbiology*. 00:B:1B.2:1B.2.1-1B.2.15.

524 Stoodley, P., Doods, I., Boyle, J.D., Lappin-Scott, H.M., 1999, Influence od hydrodynamics and
525 nutrients on biofilm structure. *J Applied Microbiology Symposium supplement*, 85, 19S-
526 28S.

527 Tolker-Nielsen, T., Sternberg, C., 2011. Growing and analyzing biofilms in flow chambers. Curr.
528 Protoc. Microbiol. Chapter 1, Unit 1B.2.

529 Trepos, R., Cervin, G., Hellio, C., Pavia, H., Stensen, W., Stensvag, K., Svendsen, J.S., Haug, T.,
530 Svenson, J. 2014, Antifouling Compounds from the sub-artic ascidian *synoicum*
531 *pulmonaria*:synoxazolidinones A and C, Pulmonarins A and B, and synthetic analogues. J. Nat.
532 Prod, 77, 2105-2113.

533 Wahl M. 1989. Marine epibiosis. I. Fouling and antifouling: some basic aspects. Mar. Ecol. Prog.
534 Ser., 58,175-189.

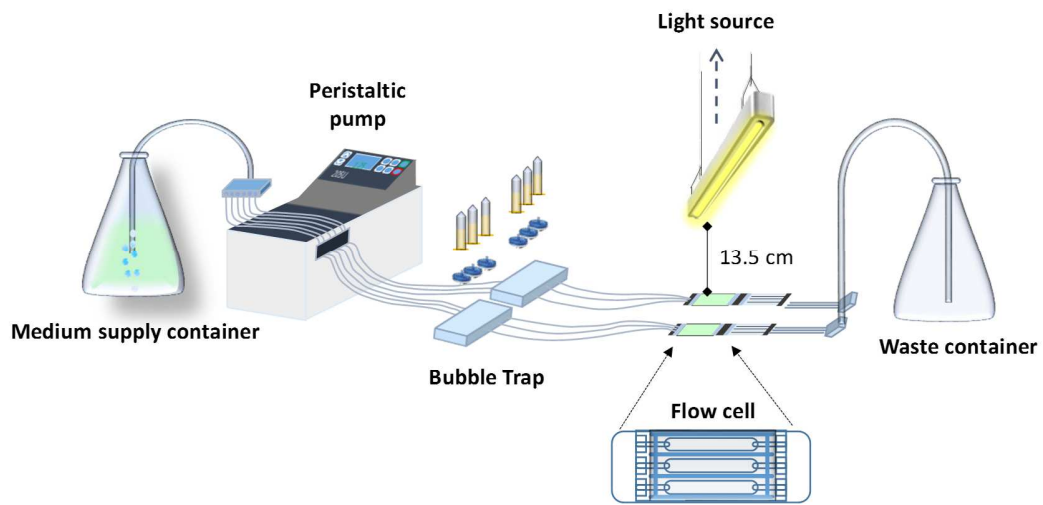
535 Xin, X., Huang, G., Zhou, X., Sun, W., Jin, C., Jiang, W., Zhao, S., 2017. Potential antifouling
536 compounds with antidaatom adhesion activities from the sponge-associated bacteria, *Bacillus*
537 *pumilus*. J Adhesion Sciences and technology 31, 1028-1043.

538 Zaouk, L., Massé, A., Bourseau, P., Taha, S., Rabiller-Baudry, M., Jubeau, S., Teychené, B., 2018.
539 Filterability of exopolysachharides solutions from the red microalga *porphyridium cruentum*
540 by tangential filtration on a polymeric membrane. Environmental Technology. DOI:
541 10.1080/09593330.2018.1523234

542 Zargiel, K.A., Swain, G.W., 2014. Static vs dynamic settlement and adhesion of diatoms to ship
543 hull coatings. Biofouling, 30, 115-129.

544
545
546

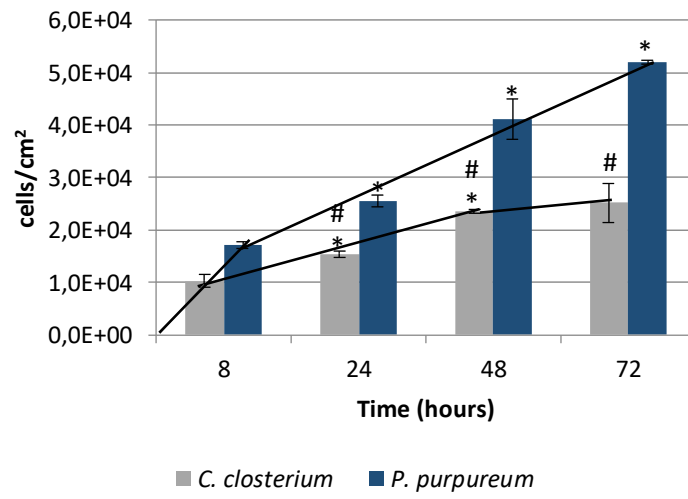
547



548

549

Figure 1. Flow cell system adapted from Tolker-Nielson and Steinberg (2011)



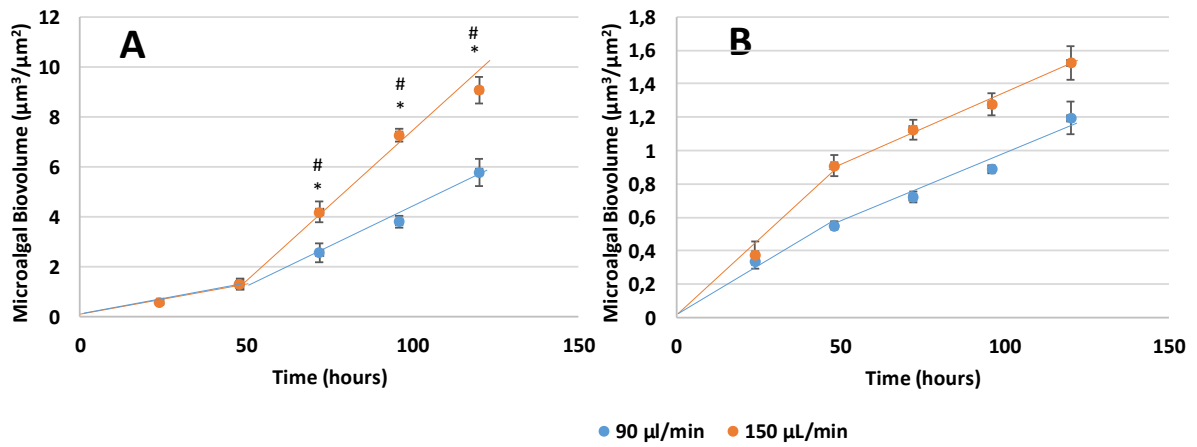
550

551 Figure 2: Adhesion kinetics on flow cell during 72h for *C. closterium* and *P. purpureum*. ANOVA
 552 *p <0.01, compared to the precedent time #p <0.01; compared between microalgae. The errors bars
 553 represent standard deviations calculated from three independent experiments.

554

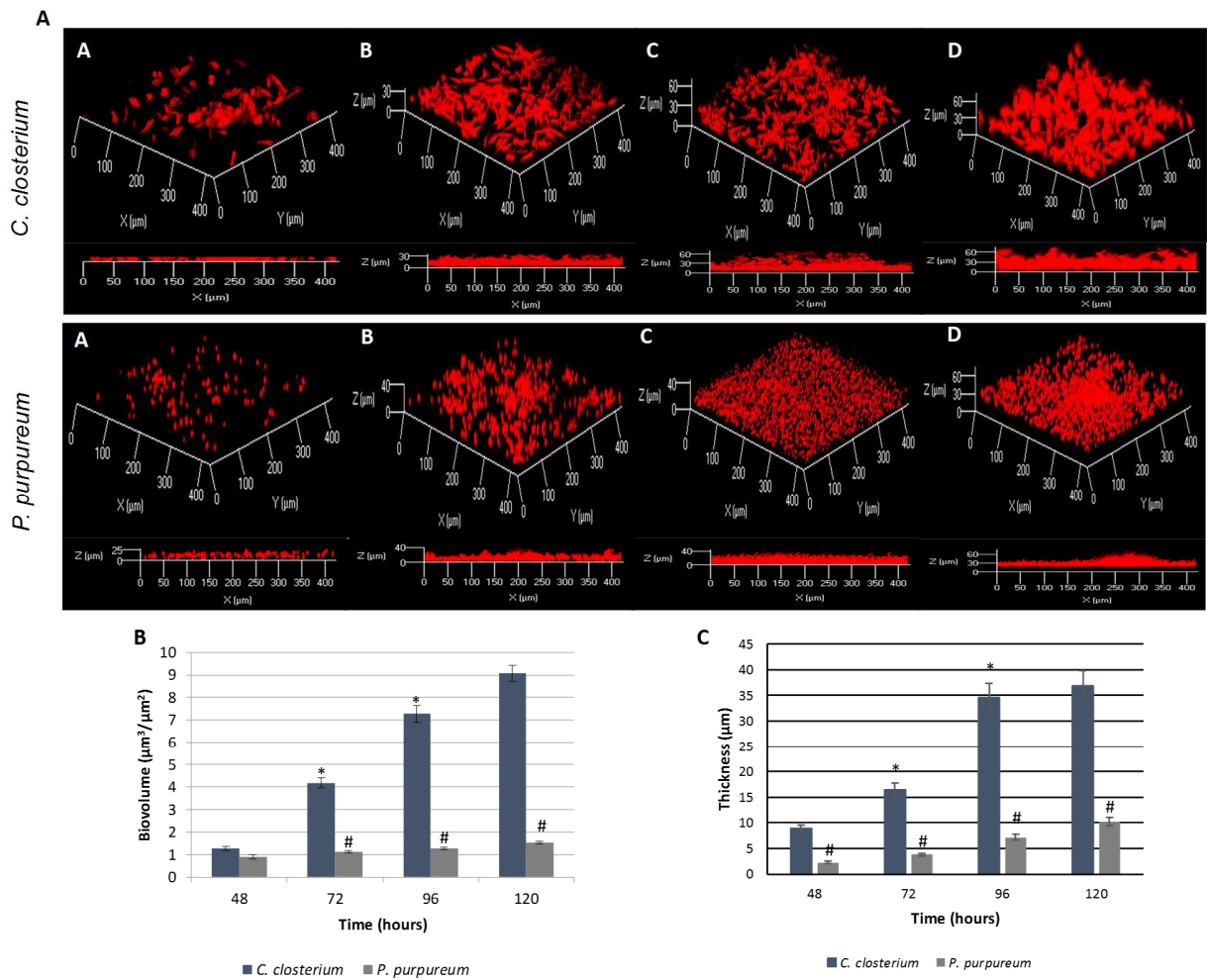
555

556



557

558 Figure 3: Effect of medium flow on microalgal biomass during biofilm maturation (A) *C.*
559 *closterium*, (B) *P. purpureum*. ANOVA * $p < 0.01$, compared to the precedent time # $p < 0.01$;
560 compared between flows. The errors bars represent standard deviations calculated from three
561 independent experiments.
562



564

565 Figure 4: (A) CLSM observations of biofilm formation pour *C. closterium* and *P. purpureum*
 566 with a flow of 150 $\mu\text{L}/\text{min}$ A. 48h, B. 72h, C. 96h, D. 120h, (B) Biovolumes and (C) Average
 567 thicknesses for *C. closterium* and *P. purpureum* during maturation stage. ANOVA, * $p < 0.01$,
 568 compared to the precedent time, # $p < 0.01$, compared between microalgae

569

570 Table 1. Overview of the classical *in vitro* method used to study antimicrobial activity of
 571 molecules and flow cells method

	Multi-well plates ^a	Flow-cells
Nutrient availability	Closed system (static)	Open system (dynamic)
Adherence	Wells (polystyrene)	Glass of coverslip
Time incubation	5 days	Between 2 hours and 6 days
Biofilm visualization	-	Direct real-time
Structural analysis	-	Analysis of structural parameters
Compound incubation	In wells	Added to the medium bottle and circulated through the flow cell for the required time

572 ^aHellio et al. 2015, Treppos et al. 2014, Reddy et al. 2017

573

574 Table 2. Comparison of data evaluated with multi-well plates and flow-cells system to evaluate
 575 bioactive compounds

	Multi-well plates	Flow-cells
Parameters	<ul style="list-style-type: none"> ▪ Planktonic growth ▪ Biofilm from planktonic and adhered cells 	<ul style="list-style-type: none"> ▪ Adhesion ▪ Biofilm from adhered cells ▪ Adhesion strength
Variables	<ul style="list-style-type: none"> ▪ Screening of compounds ▪ Concentration range 	<ul style="list-style-type: none"> ▪ One compound ▪ One concentration ▪ One strain ▪ Variability of surfaces
Results	<ul style="list-style-type: none"> ▪ Growth MIC ▪ Adhesion MIC 	<ul style="list-style-type: none"> ▪ Cell enumeration by surface unit ▪ Biofilm morphology ▪ Biovolume, biofilm thickness ▪ Adhesion strength ▪ Extracellular Polymeric Substances observation

576